Degradation of Rhodamine B by glass foam coated with WO_3 and TiO_2 under simulated solar radiation

Madalina Ivanovici[1, 2], Paulina Vlazan[1], Stefan Danica Novaconi[1], Florina Stefania Rus[1, a)]

[1] *National Institute for Research and Development in Electrochemistry and Condensed Matter, Aurel Paunescu Podeanu Street, No. 144, 300569 Timisoara, Romania*
[2] *Politehnica University of Timisoara, Piata Victoriei, No. 2, 300006 Timisoara, Romania*

[a)]Corresponding author: rusflorinastefania@gmail.com

Abstract. In this paper, a photocatalytic evaluation was carried out for several synthetized samples of glass foam coated with different amounts of TiO_2 and WO_3, respectively in order to investigate their capacity to remove Rhodamine B (RhB) from aqueous solution, under simulated solar irradiation. As the organic dyes are considered a major source of pollution to the environment, RhB was selected for this study as a dye model of organic dyes pollutants. The morphology of the glass foams impregnated with TiO_2 and WO_3 was examined by 3D laser scanning microscopy and SEM microscopy. Additionally, physical and chemical properties of the samples were determined using FT-IR and Raman spectroscopy. The artificial solar light was provided by a solar simulator Sol 2A and 20 ml RhB aqueous solution with initial concentration of 0.0015 g L^{-1} was used for each sample for the photocatalytic experiments. The degradation of RhB was determined by monitoring the absorbance of RhB solution by UV-VIS spectroscopy for 2 hours, at every 10 minutes, subsequent to the adsorption-desorption equilibrium reached in dark conditions. Enhanced photocatalytic properties were obtained for the samples of glass foams coated with TiO_2, with a maximum degradation of RhB of 92%, whereas the degradation of RhB in the presence of WO_3 fixed on glass foams reached a maximum value of 58%.

INTRODUCTION

Foam glass is a commercial material with several advantageous properties that makes it suitable for various applications especially in the construction field. Among the valuable properties, there may be mentioned low density, high mechanical stability, sound and heat insulating properties, low moisture permeability, anti-flammability, resistance to frosting, chemical and dimensionally stability [1-3]. The main disadvantage of the glass foam is the high price given by the expensive operations in the manufacturing process [4]. In this context, both the commercial and the research activities have been focused on the obtaining of the foam glass by exploitation of glass wastes [5].

In order to reduce the harming impact to the environment of the anthropogenic activities, photocatalysis is considered a promising pathway for removal of various pollutants. Numerous photocatalytic studies have been carried out on the degradation of the organic dyes as a route for treating the wastewater contaminated with dyes [6, 7]. Dyes are a major source of wastewater contamination, of which some of them shows resistance to light and temperature and are reported to have carcinogenic and mutagenic effect on various forms of life [8, 9]. Considerable amounts of dyes are coming from textile industries, where up to 20% of the dyes are discharged in the aqueous effluents, because the dyeing process is not very efficient [10].

Numerous experimental activities have been focused on photodegradation of organic dyes using semiconductors as photocatalysts, but there is a limited number of studies related to photocatalytic activity of semiconductors supported on glass foams for dyes removal [11]. In the literature, porous glass activated with different materials such as titanium oxide, zinc oxide, titanium oxide modified with silver ions have shown to possess photocatalytic properties for removal of various dyes like Rhodamine B, Methylene Blue, Orange B and Methyl Orange [12-17].

In the present study, different samples of glass foams were obtained using domestic glass waste as the main raw material and calcium carbonate ($CaCO_3$) waste from marble industry as a foaming agent. Two different semiconductor materials: titanium oxide (TiO_2) and tungsten oxide (WO_3), respectively were used as coatings for activating the glass foams for photocatalytic application regarding the organic dye removal. Therefore, TiO_2 on the glass foams and WO_3 on the glass foams were subjected to photocatalytic studies for degradation of Rhodamine B (RhB) under simulated solar light.

EXPERIMENTAL PROCEDURE

Synthesis of the samples

The raw materials used for the synthesis of glass foams are glass waste collected from household activities and $CaCO_3$ provided from marble industry. Each material was grinded and passed through sieves until a powder with particle size of 0.036 mm was obtained. The $CaCO_3$ and marble powders were mixed together with ethylene glycol (Sigma Aldrich, analytical standard). Further, the mixture is pressed resulting in formation of pastilles of different sizes, after which the pastilles were subjected to a heating treatment at temperature of 850°C, with a heating rate of 5°C/minute for 30 minutes in a furnace (SNOL 8.2/1100 LHM01). During this process, the CO_2 bubbles are formed as a result of $CaCO_3$ thermal decomposition which led to generation of pores inside the glass and in this way, the foam glass samples were obtained. The following step toward the preparation of functional foam glass consisted of coating the glass foams with photocatalytic materials: TiO_2 and WO_3, respectively. For this purpose, the glass foam samples were submerged in a slurry formed by TiO_2 (or WO_3) nanoparticles and a solvent mixture containing ethylene glycol and 2-metoxiethanol (Sigma Aldrich, analytical standard) in a molar ratio of 1:1. After this step, a heat treatment was applied for solvent evaporation at 80°C. In order to achieve different quantities of TiO_2 (or WO_3) coated on the glass foams, the impregnation procedure was repeated several times. The nanoparticles of TiO_2 and WO_3 were obtained in previous studies by hydrothermal method (for TiO_2) and combustion method (for WO_3).

Characterization techniques

The morphology of the glass foam samples coated with WO_3 and TiO_2 were determined by scanning electronic microscope (SEM), Inspect S (FEI Company, Eindhoven, Netherland). Additional analyses for pores and surface configuration were performed with a 3D laser scanning microscope OLS 4000 Lext Olympus. FT-IR characterization was used for providing qualitative analyses of the uncoated glass foams and of the glass foam coated with TiO_2 and WO_3, respectively before and after photocatalytic experiments. FT-IR spectrometer Vertex 70 (Bruker, Germany) was used in the range of 400-4000 cm^{-1} using 128 scans and a resolution of 8 cm^{-1}. Complementary, Raman spectra were obtained for glass foam impregnated with TiO_2 and WO_3 with scanning probe microscopy system: Multi Probe Imaging –MultiView 1000^{TM} system (Nanonics Imaging, Israel).

Photocatalytic degradation experiment

The photocatalytic tests were carried out in glass container using 20 ml of aqueous solution of Rhodamine B with an initial concentration of 1.5 mg L^{-1}. Each sample was immersed in the solution and subjected to a stirring process, in dark conditions, until the adsorption-desorption equilibrium between the sample and the solution was achieved. After this step, the system consisting of sample and the RhB solution was irradiated by artificial sun light by placing the container under the solar simulator (Sol2A 94042A, Oriel Instruments/Newport Corporation) for two hours. The ultraviolet fraction of simulated solar radiation were measured with a UVA/UVB radiation detector (PCE-UV34) indicating a irradiance power of 1.11 mW cm^{-2}, and the visible fraction was measured with solar analyzer (SOLAR-4000 Sensor provided by Beha-Amprobe) indicating a irradiance power of 840 W m^{-2}.

The degradation measurements were performed by using a fiber optic UV-VIS spectrophotometer. In this sense, an experimental setup was settled by connecting a cuvette holder, which serves as support for a quartz cuvette, with the light source (LS-1 from Ocean Optics), at one side and with UV-VIS spectrophotometer (portable Jaz spectrometer from Ocean Optics) at the other side. In the adsorption-desorption stage, small volumes of RhB aqueous solution were collected at every 30 minutes and introduced in the cuvette in order to record the absorbance value of the dye solution, until the absorbance remained constant. Also, during the two hours of light exposure of the sample-solution system, the absorbance of RhB solution was monitored at every 10 minutes.

RESULTS AND DISCUSSION

Characterization methods

In Fig. 1, it could be seen the morphological and the distribution of semiconductors nanoparticles on the glass foam support determined by scanning electronic microscopy. In the Fig. 1 (a), several TiO_2 nanoparticles are identified on analyzed glass foam surface and the uncovered area reveals small pores of different sizes within its structure. Figure 1 (b) illustrates that WO_3 nanoparticles were dispersed on the entire analyzed surface of the glass foam, of which the most of the nanoparticles were present in spherical shape, but there are also nanoparticles with irregular shape [18].

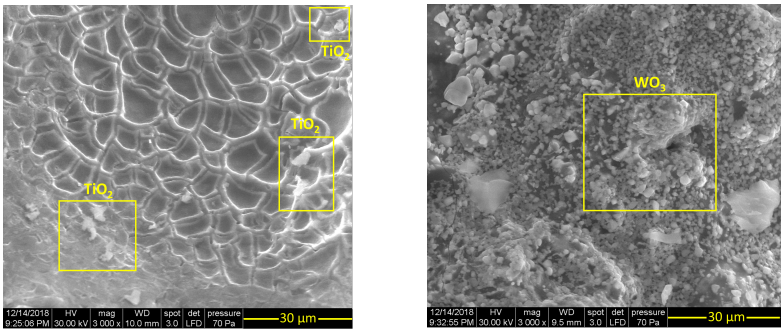

(a) (b)

FIGURE 1. SEM images of the glass foams coated with (a) TiO_2 and (b) WO_3 nanoparticles

Additional information related to the surface topography of the samples could be identified in 3D laser scanning microscope images (Fig. 2), for which higher surfaces compared to SEM images were analyzed.

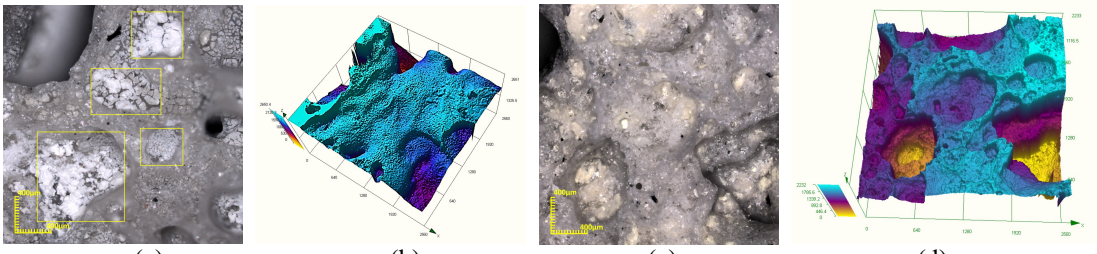

(a) (b) (c) (d)

FIGURE 2. Laser scanning microscopy images for the glass foams coated with TiO_2 ((a)-2D image and (b)-3D image) and with WO_3 ((c)-2D image and (d)-3D image)

In Fig. 2 (a), a clearer image of TiO_2 deposition is illustrated on the marked zones. Furthermore, by correlation with 3D image (Fig. 2 (b)), the deposition of TiO_2 inside the glass foam pores is confirmed. Similarly to TiO_2 coated on the glass foam, in Fig. 2 (c), the glowing yellow spots represent the WO_3 nanoparticles coated on the surface of the glass foams and the 3D representation (Fig. 2 (d)) prove the presence of WO_3 inside the pores. The pores displayed in the 3D images present different shapes (heights and widths) which indicates a heterogeneous porosity of the glass foams.

FT-IR spectra of the foam glass simple samples and the coated with WO_3 and TiO_2, respectively before and after photocatalytic experiments has been recorded in the 400 to 4000 cm^{-1} spectra range and is shown in Fig. 3. The bands present at around 3430 and 1630 cm^{-1} are associated to water (OH group and H_2O group) adsorption on the surface of the analyzed samples [19]. The two bands of low intensity from 2859 and 2928 cm^{-1} can be attributed to the stretching vibration of the – CH groups and the band at 2360 cm^{-1} corresponds to CO_2 [20]. The low frequency bending vibration is observable at ~1630 cm^{-1} corresponding to Me–OH planes and the bands around 1400 cm^{-1} can be attributed as antisymmetric and symmetric CO_2 stretching modes. In Fig. 3 (a) red line corresponding for the foam glass coated with WO_3 indicates a strong stretching vibration (W–O–W) response in the inorganic compound visible at around 800 cm^{-1} [21].

All spectra of the samples show a strong and broadband between 900-1100 cm^{-1} attributed to the Si–O stretching vibrations, and at ~780 and 470 cm^{-1} assigned to Si–O–Al (octahedral Al) and Si–O–Si bending vibrations, respectively.

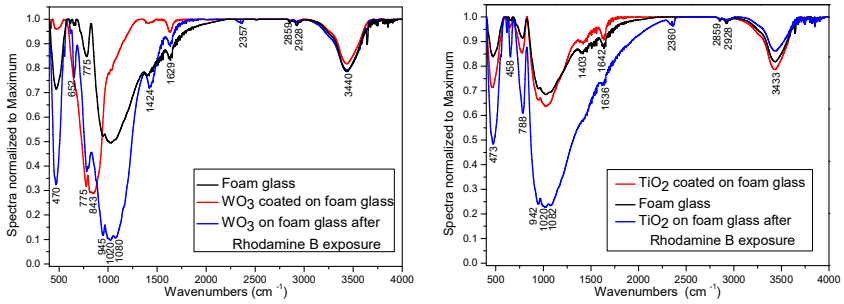

(a) (b)

FIGURE 3. FT-IR spectrum of (a) the glass foam coated with WO_3 before (red line) and after the photocatalytic experiment (blue line) and of the uncoated foam glass (black line) and (b) of the foam glass coated with TiO_2 before (red line) and after (blue line) photocatalytic experiments and of the uncoated foam glass (black line)

Also the spectra of transition metal oxides show Me–O stretching and bending as well as OH bending absorptions in the 1300–400 cm^{-1} range [22]. The FTIR spectra of the foam glass after photocatalytic experiment shows a significant increase of the bands intensity as well as a slight shift of the spectra towards higher wavelengths. Moreover, a decrease in the intensity of bands corresponding to water molecules indicates replacement of the water molecules with the dye molecules. These band shifts are attributed to the interaction of the RhB molecules with the metal oxides in the samples [23].

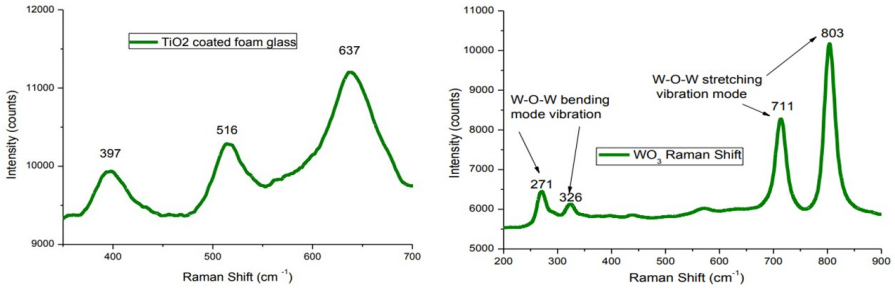

(a) (b)

FIGURE 4. Raman analyses for glass foam coated with (a) TiO_2 and (b) WO_3

Micro Raman spectroscopy using laser wavelength of 532 nm has been employed for providing information regarding the vibrational modes and crystalline phases of TiO_2 and WO_3 (Fig. 4). The anatase phases of TiO_2 could be sensitively identified by Raman spectroscopy based on their Raman spectra. In Fig. 4 (a), three well defined peaks were identified: 397 cm^{-1} (B1g), 517 cm^{-1} (A1g) and 637 cm^{-1} (Eg) corresponding to the anatase TiO_2 active bands [24]. Figure 4 (b) shows four vibrational modes of the crystalline phase of WO_3. The intense modes at 803 and 711 cm^{-1} are assigned to the stretching vibration of the tungsten and adjoining oxygen atoms, ν (O–W–O), and the modes exhibited at 271 and, respectively 326 cm^{-1} are attributed to the bending mode δ (O–W–O) [25].

Photocatalytic activity

The behavior of the RhB removal during the adsorption and the photocatalysis process for both TiO_2 and WO_3 fixed on the glass foam samples is presented in Fig. 5. The amounts of the coated semiconductor materials and the sizes of the samples in terms of the irradiated areas are showed in Table 1. In Fig. 5(a) it could be seen that sample P1_TiO_2 reached the adsorption-desorption equilibrium in the shortest time, so that only after 30 minutes, the absorbance of RhB decreased approximately 7.5%, after which the absorbance remained constant. It could be noticed that as the size of the samples subjected to the adsorption stage was increasing, the removal of RhB from

aqueous solution was enhanced. Therefore, the sample P2_TiO_2 reached a decrease of the RhB absorbance around 33% in 2 hours and for the sample P3_TiO_2, the RhB absorbance decreased approx. 39% in 90 minutes.

The catalyzed reaction of the degradation of Rhodamine B is promoted by the solar radiation. As the radiation provided by solar simulator reached only one side of the samples, a major factor that was affecting the dye degradation performance is represented by the irradiated surface of the samples. In Fig. 5(a), S1 is representing the illuminated surface corresponding to P1_TiO_2. For this sample, the RhB degradation during photocatalysis went slowly increasing from approximately 7.5% to 26%. With an irradiated surface approximately 6 times larger than of P1_TiO_2, P2_TiO_2 led to the RhB removal of approximately 62%, around 2.4 times more than the first sample. The best results were obtained for the P3_TiO_2, with a surface of 9 times larger than of P1_TiO_2 for which the absorbance of the solution decreased close to 0.02, leading to RhB removal of around 92%, 3.5 times more than the first sample. It could be concluded that enhanced photocatalytic activities were obtained for the samples with higher irradiated surfaces.

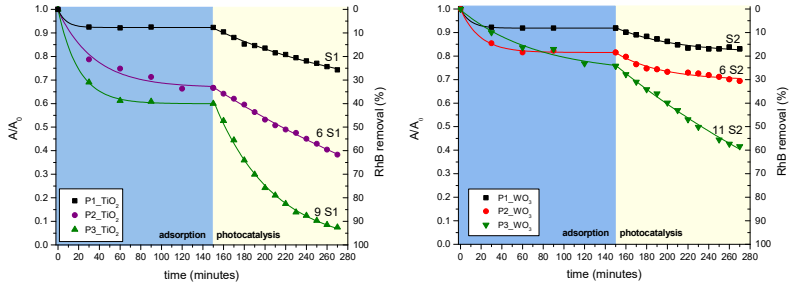

(a) (b)

FIGURE 5. Degradation of RhB by the foam glass samples coated with (a) TiO_2 and (b) WO_3

In Fig. 5 (b), the RhB removal by WO_3 fixed on the glass foams is represented and the S2 is the surface of P1_WO_3. Similarly to TiO_2 on glass foams, P1_WO_3 attained the stabilization of the adsorption-desorption process after 30 minutes, for which the RhB absorbance decreased around 8% from the initial value. The larger size samples were, the adsorption-desorption equilibrium was achieved in a longer time, in one hour for P2_WO_3 with RhB removal of 18 % and in 150 minutes for P3_WO_3 with removal of RhB of 24%. In the photocatalysis stage, the degradation of RhB increased from 8% to 17% for P1_WO_3 and from 18% to 31% for P2_WO_3. P3_WO_3 generated the highest degradation of 58%. During the each phase of the experiments: the adsorption and the photocatalysis, the absorbance of RhB showed exponential decrease for all tested samples.

TABLE 1. The amounts of the TiO_2 and WO_3 fixed on the glass foams and the irradiated surfaces of the tested samples

Sample code	Mass of oxide coated on glass foam [mg]	Irradiated surface of sample [cm^2]	Sample code	Mass of oxide coated on glass foam [mg]	Irradiated surface of sample [cm^2]
P1_TiO_2	8.7	0.785	P1_WO_3	66.1	0.785
P2_TiO_2	19.4	4.524	P2_WO_3	102.3	4.909
P3_TiO_2	60.2	7.069	P3_WO_3	203	8.545

Despite the fact that the irradiated surfaces of WO_3 fixed on glass foams are proximate or even bigger than the irradiated surfaces of the glass foams coated with TiO_2 and that the mass of WO_3 fixed on glass foams are higher than the mass of coated TiO_2, the glass foams impregnated with TiO_2 presented higher RhB degradation.

The penetration of light through the pores and the interaction of the light with the photocatalytic material fixed on the glass foams are factors that influence the photocatalytic properties of the samples. In this sense, further investigation related to porosity of the samples and distribution of the TiO_2 and WO_3 on the glass foams is needed to be done for a comprehensive correlation between the morphologies and the capacities of the samples for removing RhB.

CONCLUSION

In this study the potential of glass foams for environmental application has been pointed out. For this purpose, two aspects were employed: the usage of wastes as raw materials for the glass foam preparation and the removal of

dye pollutants (Rhodamine B) under simulated solar light after a previous step of coating the glass foam samples with photocatalytic materials (TiO_2 and WO_3).

SEM and the laser scanning images showed the formation of the pores of different sizes within the structure of glass foam and the distribution of the TiO_2 and WO_3 on the surface of glass foams. Raman and FT-IR analyses emphasized the presence of photocatalytic materials in their crystalline form and the main interactions ascribed to the metal-oxygen bonds (e.g. W–O, Si–O, Al–O) and to the water adsorbed on the surface of samples.

In the photocatalytic experiments, the removal of RhB from aqueous solution was achieved as a result of the adsorption and solar irradiation exposure stages. As the main factor affecting the photocatalytic degradation was the irradiated surface of the sample, it could be concluded that photocatalytic activities of the TiO_2 and WO_3, respectively fixed on the foam glass was enhanced with the increasing illuminated area of the samples. The glass foams coated with TiO_2 showed a higher removal of RhB than the glass foams coated with WO_3 even if the amounts of the coated WO_3 were higher and the illuminated surfaces were similar or even larger for the foam glass samples impregnated with WO_3.

ACKNOWLEDGMENTS

This research is a part of the project PN-III-P1-1.2-PCCDI-2017-0391/CIA_CLIM-Smart buildings adaptable to the climate change effects, granted by Romanian Ministry of Research and Innovation, CCCDI–UEFISCDI.

REFERENCES

1. E. A. Yatsenko, V. A. Smolii, B. M. Goltsman and A. S. Kosarev, J. Int. Sci. Publ.: Mater. Methods Technol. **8**, 54-61 (2014).
2. A. M. Papadopoulos, Energ. Buildings **37**, 77-86 (2005).
3. J. Bai, X. Yang, S. Xu, W. Jing and J. Yang, Matter. Let. **136**, 52-54 (2016).
4. J. König, R. R. Petersen and Y. Yue, Ceram. Int. **41**, 9793-9800 (2015).
5. H. R. Fernandes, D. U. Tulyaganov and J. M. F. Ferreira, Ceram. Int. **35**, 229-235 (2009).
6. F. M. D. Chequer, G. A. R. de Oliveira, E. R. A. Ferraz, J. C. Cardoso, M. V. B. Zanoni and D. P. de Oliveira, "Textile Dyes: Dyeing Process and Environmental Impact" in *Eco-Friendly Textile Dyeing and Finishing*, edited by M. Günay (IntechOpen, 2013), pp. 151-176.
7. R. Ameta, S. Benjamin, A. Ameta and S. C. Ameta, Mater. Sci. Forum **734**, 247-272 (2012).
8. E. Forgacs, T. Crestile and G. Oros, Environ. Int. **30**, 953-971 (2004).
9. C. O'Neill, F. R. Hawkess, D. L. Hawkess, N. D. Lourenco, H. M. Pinheiro and W. Delee, J. Chem. Technol. Biotechnol. **74**, 1009–1018 (1999).
10. P. Cooper, *Color in dyehouse effluent* (Society of Dyers and Colourists, Bradford, 1995).
11. K. Rajeshwar, M. E. Osugi, W. Chanmanee, C. R. Chenthamarakshan, M. V. B. Zanoni, P. Kajitvichyanukul and R. Krishnan-Ayera, J. Photoch. Photobio. C **9**, 171–192 (2008).
12. Y. Chen, C. Shen, J. Wang, G. Xiao and G. Luo, ACS Sustainable Chem. Eng. **6**, 13276-13286 (2018).
13. G. Falk, Ê. L. Machado, D. Rodríguez, W. Acchar and A. Rodriguez, Mater. Sci. Forum **820**, 594-599 (2015).
14. E. M. Rangel, C. C. Melo and F. Machado, Bol. Soc. Esp. Ceram. V. **58**, 134-140 (2019).
15. C. Shen, Y. J. Wang, J. H. Xu and G. S. Luo, Chem. Eng. J. **209**, 478–485 (2012).
16. Q. Xu, J. Zeng, X. Li, J. Xu and X. Liu, RSC Advances **6**, (2016).
17. T. Yazawa, F. Machida, N. Kubo and T. Jin, Ceram. Int. **35**, 3321-3325 (2009).
18. M. Alaei, A. R. Mahjoub and A. Rashidi, Iran. J. Chem. Chem. Eng. **31**, 31-36 (2012).
19. C. Y. Heah, H. Kamarudin, A. M. M. Al Bakri, M. Bnhussain, M. Luqman, I. Khairul Nizar, C. M. Ruzaidi and Y. M. Liew, Constr. Build. Mater **35**, 912-922 (2012).
20. J. D'Angelo, ALDEQ **18**, 34-38 (2004).
21. V. B. Kumar and D. Mohanta, B. Mater. Sci. **34**, 435-442 (2011).
22. J. Madejova, Vib. Spectrosc. **31**, 1–10 (2003).
23. S. Mukhtar, M. Liu, J. Han and W. Gao, Chinese Phys. B **26**, 058202 (2017).
24. T. Oksaka, F. Izumi and Y. Fujiki, J. Raman Spectrosc. **7**, 321-324 (1978).
25. M. F. Daniel, B. Desbat, J. C. Lassegues, B. Gerand and M. Figlarz, J. Solid State Chem. **67**, 235-247 (1987).